J Math Chem (2009) 46:763–769
DOI 10.1007/s10910-009-9545-1

ORIGINAL PAPER

Modeling the dissociation of carbon dioxide and methane hydrate using the phase field theory

A. Svandal · B. Kvamme

Received: 8 November 2007 / Accepted: 30 September 2008 / Published online: 19 July 2009

Abstract Hydrate that is exposed to fluid phases which are undersaturated with respect to equilibrium with the hydrate will dissociate due to gradients in chemical potential. Kinetic rates of methane hydrate dissociation towards pure water and seawater is important relative to hydrate reservoirs that are partly exposed towards the ocean floor. Corresponding results for carbon dioxide hydrate is important relative to hydrate sealing effects related to storage of carbon dioxide in cold aquifers. In this work we apply a phase field theory to the prediction of carbon dioxide hydrate and methane hydrate dissociation towards pure water at various conditions, some of which are inside and some which are outside the stability regions of the hydrates with respect to temperature and pressure. As expected from the differences in water solubility the methane hydrate dissolves significantly slower towards pure water than carbon dioxide hydrate.

Keywords Gas hydrate · Phase-field theory · Carbon dioxide · Dissociation · Methane

1 Introduction

Gas hydrates are crystalline structures in which water forms cavities that enclathrates small non-polar molecules, so called guest molecules, like for instance CO_2 or CH_4. Macroscopically the structure looks similar to ice or snow but unlike ice these hydrates are also stable at temperatures above 0 °C. The enclathrated molecules stabilize the hydrate through their volume and interactions with the water molecules which

A. Svandal · B. Kvamme (✉)
Department of Physics and Technology, University of Bergen,
Allègaten 55, 5007 Bergen, Norway
e-mail: bjorn.kvamme@ift.uib.no

constitutes the cavity walls. Natural gas hydrate reservoirs which are partly exposed towards the seafloor will dissociate due to gradients in chemical potentials between the enclathrated guest molecules and chemical potentials of the same components in the seawater outside the hydrate structure. As a greenhouse gas methane is in the order of 25 times more aggressive than CO_2. Worldwide there are many regions of hydrate reservoirs which are partly exposed towards the seafloor and constantly leaking methane. Regions of the Bermuda triangle are probably the most famous due to the theories of sudden release of huge methane bubbles that have caused ships to sink. It is therefore an important global challenge to be able to make acceptable predictions of the dissociation flux of methane from such exposed reservoirs, and to be able to model the corresponding net flux of methane that escapes to the atmosphere after biological consumption and conversion through inorganic and organic reactions. In a more general sense it is not likely that any hydrate reservoirs are thermodynamically stable in a rigorous thermodynamic sense. Most hydrate reservoirs are trapped by clay layers and kept in a state of extremely slow dissociation dynamics due to slow transport of dissociated molecules through clay layers above the hydrate. The stability of CO_2 storage in cold reservoirs may be enhanced through the formation of hydrate films. These hydrate films will form rapidly on the CO_2/water interface and create a more or less closed membrane which reduces the transport of water and CO_2 across the hydrate film. Eventually this will lead to a dynamic situation where the dissociation of hydrate towards the aqueous phase above will be the rate limiting process that determines the net flux of CO_2 through the hydrate sealing.

2 Phase field theory

A phase field theory has previously been applied to describe the formation of CO_2 and CH_4 hydrate in aqueous solutions [1–3]. In this paper the theory is applied to model the dissociation of the hydrates. The solidification of hydrate is described in terms of the scalar phase field ϕ and the local solute concentration c. The field ϕ is a structural order parameter assuming the values $\phi = 0$ in the solid and $\phi = 1$ in the liquid. Intermediate values correspond to the interface between the two phases. Only a short review of the model will be given here. Full details of the derivation and numerical methods can be found elsewhere [3–8]. The starting point is a free energy functional

$$F = \int dr^3 \left[\frac{1}{2} \varepsilon^2 T \, |\nabla \phi|^2 + f \, (\phi, c) \right], \tag{1}$$

with ε being a model constant, T is the temperature and the integration is over the system volume. In this paper we use c for concentration with units moles per volume and the mole fraction of the guest is termed x and is dimensionless. Assuming equal molar volume for the two components the following relation: $c = x/v_m$ can be applied, where v_m is the average molar volume. The range of the thermal fluctuations is on the order of the interfacial thickness and, accordingly, ε may be fixed from knowledge of this thickness. The gradient term is a correction to the local free energy density $f(\phi, c)$. To ensure minimization of the free energy and conservation of mass,

the governing equations can be written as

$$\dot{\phi} = -M_\phi \frac{\delta F}{\delta \phi} \tag{2}$$

$$\dot{c} = \nabla \cdot \left(M_c \nabla \frac{\delta F}{\delta c} \right), \tag{3}$$

where M_c and M_ϕ are the mobilities associated with coarse-grained equation of motion, which in turn are related to their microscopic counterparts. The local free energy density is assumed to have the form

$$f(\phi, c) = wTg(\phi) + [1 - p(\phi)]\, f_S(c) + p(\phi) f_L(c) \tag{4}$$

where the "double well" and "interpolation" functions have the forms which emerge from the thermodynamically consistent formulation of the theory [8]. The parameter w is proportional to the interfacial free energy and can be deduced from experimental measurements or predicted from molecular simulations of representative model systems. For this work the applied value used was the experimental value for water/ice reported as 29.1 mJ/m^2 [9]. The thermodynamic functions of the hydrate and the aqueous solutions have been determined using solubility data and molecular dynamics simulations. Here only the form of the functions is given. A full description of the derivation can be found in Ref. [10]. The free energy functions in Eq. 4, for a phase P, have the general form:

$$v_m f_P = x \cdot \mu_c + (1 - x)\mu_w, \tag{5}$$

where μ_c and μ_w are the chemical potentials of the guest molecule and water in that phase. For the aqueous solution we use

$$\mu_c = \mu_c^\infty(T) + RT \ln(x\gamma_c). \tag{6}$$

Here $\mu^\infty{}_c(T)$ is the chemical potential at infinite dilution of component c in water. R is the universal gas constant and γ_c is the activity coefficient of the guest in an aqueous solution in the asymmetric convention (γ_{CO_2} is unity in the limit as x goes to zero). For water we have

$$\mu_w = \mu_w^{\text{pure}}(T) + RT \ln((1 - x)\gamma_w). \tag{7}$$

Here $\mu^{\text{pure}}{}_w(T)$ is the chemical potential of pure water. The activity coefficient of water can be obtained through the Gibbs–Duhem relation. The expression for the chemical potential of water in hydrate with only one type of guest molecule is

$$\mu_w^H = \mu_w^{0,H} + v_m (P - P_0) - \sum_j RT v_j \ln\left(1 + h_j\right). \tag{8}$$

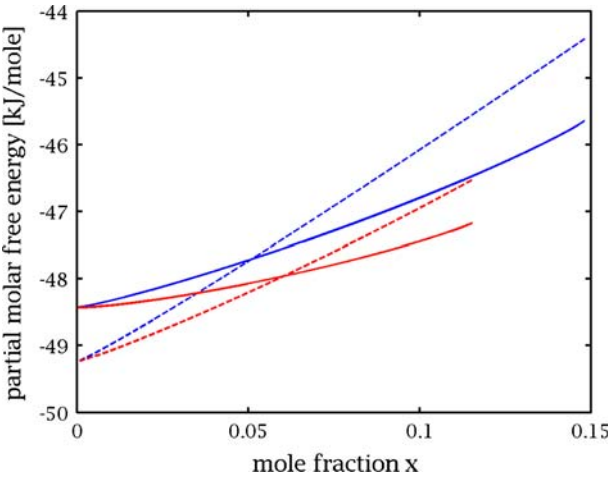

Fig. 1 Free energies of hydrate (*solid line*) and the aqueous solution (*dashed line*) as a function of the mole fraction at 40 bars and 1 °C. *Red lines* are the carbon dioxide system, and the *blue lines* are for the methane system

Here ${\mu_w}^{0,H}$ is the chemical potential for water in an empty hydrate structure. The sum is over small and large cavities, where v_j is the number of type j cavities per water molecule. h_j is the cavity partition function given as $h_j/(1+h_s+h_l) = x_j/(v_L(1-x_j))$, where x_j is the molar fraction with respect to cavity j only and subscript s and l refers to small and large cavities respectively. The chemical potential for the guest molecule in hydrate can be expressed in terms of the cavity partition function as

$$\mu_k^H = \Delta g_{cj}^{\text{inc}}(T) + RT \ln\left(h_{cj}\right), \tag{9}$$

Here ${\Delta g_{c,j}}^{\text{inc}}$ is the free energy of inclusion of guest molecule c in cavity j. The total free energy for each phase and each component are shown in Fig. 1.

3 Hydrate dissociation simulations

The model has been implemented with a narrow 2D planar geometry, simulating dissociation of a planar front. The temperature is chosen to be 1 °C, which is a realistic temperature for cold reservoirs and the low seafloor temperatures which are typical for regions outside coast of the northern parts of Norway. Simulations have been conducted at 10 and 40 bars. The latter pressure represents 400 m depth, which is a typical sea floor depth and is inside the hydrate stability region. No flux boundary conditions at the walls were assumed and the grid resolution used was 0.1 nm. The time step was 0.8×10^{-12} s. Initially a pure water solution and a hydrate film with thickness 16 nm were assumed. The movement of the front was tracked by following the $\phi = 0.5$ value. In Fig. 2 simulations of carbon dioxide and methane hydrate dissociation is shown at the two different pressures. The methane dissociation rate is much slower than for carbon dioxide hydrate. This can be explained by the much lower solubility

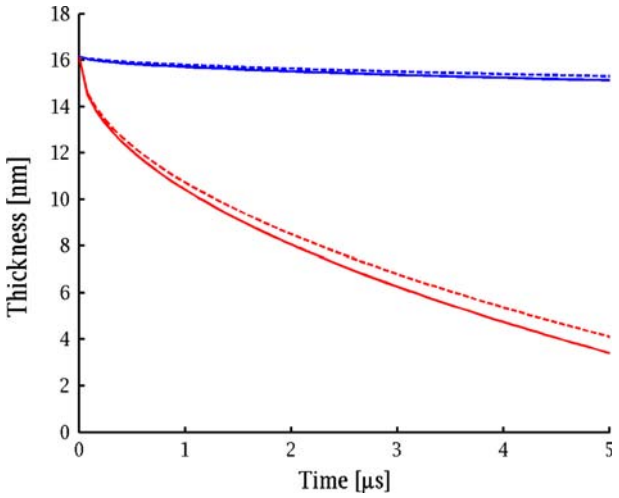

Fig. 2 Thickness of the hydrate film as a function of time for the dissociation of carbon dioxide hydrate (*red*), and methane hydrate (*blue*). *Dashed line* is 40 bars, *solid line* is 10 bars

of methane in water in agreement with previous results and discussions in Ref. [1,2], that the controlling mechanism for these systems is the chemical diffusion.

In the paper by Tohidi et al. [11] hydrate dissociation are studied experimentally for both CH_4 and CO_2, although no rates where reported. The CH_4 hydrate was observed to dissociate into bubbles while CO_2 dissolved only into the aqueous solution even at conditions far outside the hydrate stability. The transport of bubbles of CH_4 will be governed by hydrodynamics and is assumed to be faster than the diffusion. This opens for a faster rate of dissociation than predicted by Fig. 2. We have not included hydrodynamic effects into our simulations, but some simplified considerations may be conducted. Considering the dissociation of a hydrate film we can estimate how much hydrate has to be melted to yield one molecule of gas. With a mole fraction of 0.132 in the hydrate there will be 1 guest molecule per $2.3 \times 10^{-28}\,\mathrm{m}^3$, which corresponds to a box with sides 0.61 nm. Melting 0.61 nm of hydrate would then correspond to a layer of guest molecules in the aqueous solution one molecule thick. If we then assume that these molecules agglomerate and disappear the dissociation rate can be estimated from the time it takes to dissociate one molecule which can be read from Fig. 2 to be 2.8 μs. With the CH_4 disappearing in a bubble we are back to the initial situation with hydrate dissociating towards pure water, which in this simplified picture will be a cyclic process. Using these numbers we obtain a dissociation rate of 0.2 mm/s which is a reasonable number relative to experimental time scales.

With the inclusion of a concentration gradient to the free energy functional we can simulate a three phase system with the aid of only one phase field, and with a thermodynamic function of the liquid phase as presented in [10].

$$F = \int dr^3 \left[\frac{1}{2}\varepsilon_\phi^2 T\,|\nabla\phi|^2 + \frac{1}{2}\varepsilon_c^2 T\,|\nabla c|^2 + f\,(\phi, c) \right] \tag{10}$$

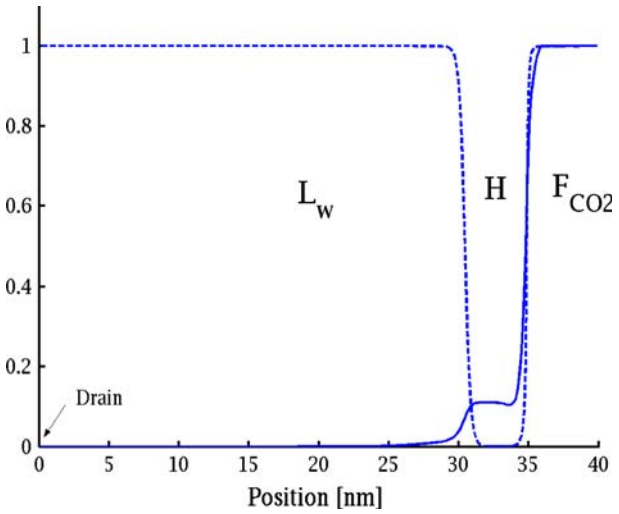

Fig. 3 Phase field (*dashed line*) and concentration profile (*solid line*) for dissociation of CO_2 through a hydrate film. L_w, liquid water phase; H, Solid hydrate; F_{CO_2}, Fluid CO_2

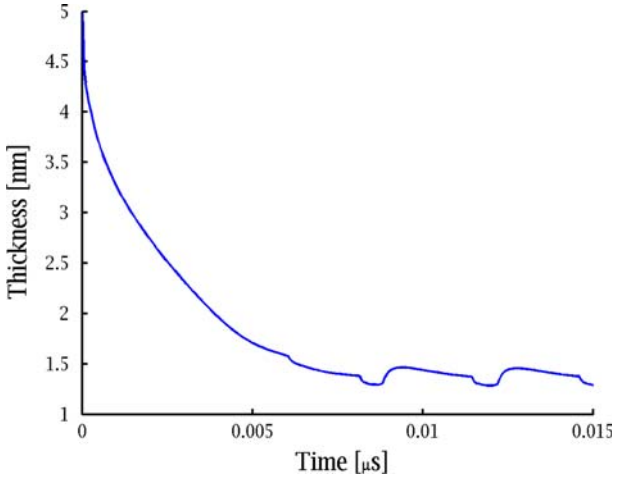

Fig. 4 Hydrate film thickness as a function of time

The ε_c parameter has been estimated to be about 40 times larger than ε_ϕ. Related to the scenario of a rising plume we now simulate a pure CO_2 phase exposed towards pure water with a hydrate film in between as pictured in Fig. 3.

For the simulations to be feasible we include a CO_2 drain in the left wall so that the CO_2 will not accumulate in the aqueous phase. The hydrate film will initially melt until some kind of temporary stable state is attained where the flux of CO_2 through the hydrate film equals the flux in the liquid. The film will then approach constant thickness until there is no more CO_2 left in the fluid phase. The thickness of the hydrate film is plotted in Fig. 4. The oscillations are due to numerical effects and are on the

order of the spatial resolution. The thickness of the film is directly proportional to the distance from the water/hydrate interface to the drain according to Fick's law. This distance can be related to a laminar diffusion layer, a term often encountered in kinetic models of hydrate growth, see for instance Ref. [12].

The presence of a hydrate film will considerably restrict the flux of CO_2 from escaping a storage reservoir.

4 Conclusions

Phase field theory simulations have been applied to model the dissociation of CH_4 and CH_2 exposed towards pure water. Presently there are no experimental data available for direct comparisons to the predictions presented here and the main purpose of this paper has been to demonstrate the approach and the corresponding parameterization. As expected relative to the differences in solubility of the two components in water the kinetic rates of CO_2 hydrate dissociation is larger than that of CH_4 hydrate. The dissociation rate of CH_4 can however be considerably higher if the process involves the generation of CH_4 bubbles. The sealing effect of a sealing hydrate film between a CO_2 plume pure water are also investigated.

Acknowledgments Financial support from the Norwegian Research Council through project 101204, and from Conoco-Phillips, is highly appreciated. We thank Làszlò Gránàsy for sharing his experience on the phase field theory. The simulations in this work are based on his phase field code.

References

1. A. Svandal, B. Kvamme, L. Gránàsy, T. Pusztai, The influence of diffusion on hydrate growth. J. Phase. Equilib. Diff. **26**(5), 534–538 (2005)
2. A. Svandal, B. Kvamme, L. Gránàsy, T. Pusztai, T. Buanes, J. Hove, The phase field theory applied to CO_2 and CH_4 hydrate. J. Cryst. Growth **287**, 486–490 (2006)
3. B. Kvamme, A. Graue, E. Aspenes, T. Kuznetsova, L. Gránàsy, G. Tòth, T. Pusztai, G. Tegze, Kinetics of solid hydrate formation by carbon dioxide; phase field theory of hydrate nucleation and magnetic resonance imaging. Phys. Chem. Chem. Phys. **6**, 2327 (2004)
4. L. Gránàsy, T. Börzsönyi, T. Pusztai, Nucleation and bulk crystallization in binary phase field theory. Phys. Rev. Lett. **88**, 206105 (2002)
5. L. Gránàsy, T. Pusztai, J.A. Warren, Modeling polycrystalline solidification using phase field theory. J. Phys. Condens. Mater. **16**, R1205–R1235 (2004)
6. L. Gránàsy, T. Pusztai, T. Börzsönyi, J.A. Warren, J.F. Douglas, A general mechanism of polycrystalline growth. Nat. Mater. **3**, 645–650 (2004)
7. J.A. Warren, W.J. Boettinger, Prediction of dendritic growth and microsegragation patterns in a binary alloy using the phase-field method. Acta. Metall. Mater. **43**, 689–703 (1995)
8. S.L. Wang, R.F. Sekerka, A.A. Wheeler, B.T. Murray, S.R. Coriell, R.J. Braun, G.B. McFadden, Thermodynamically-consistent phase-field models for solidification. Phys. D **69**, 189–200 (1993)
9. S.C. Hardy, A grain boundary groove measurement of the surface tension between ice and water. Philos. Mag. **35**, 471 (1977)
10. A. Svandal, T. Kuznetsova, B. Kvamme, Thermodynamic properties and phase transitions in the $H_2O/CO_2/CH_4$ system. Phys. Chem. Chem. Phys. **8**, 1707–1713 (2006)
11. B. Tohidi, R. Anderson, M.B. Clenell, R.W. Burgass, A.B. Biderkab, Visual observation of a gas-hydrateformation and dissociation in synthetic porous media by means of glass micromodels. Geology **29**, 867–870 (2001)
12. P. Skovborg, P. Rasmussen, A mass transport limited model for the growth of methane and ethane gas hydrates. Chem. Eng. Sci. **49**, 1131–1143 (1994)